WOOD RESEARCH doi.org/10.37763/wr.1336-4561/67.6.966978
e-ISSN 2729-8906
67(6): 2022 966-978 pp.

STUDY ON THE DISPERSION CHARACTERISTICS OF WOOD ACOUSTIC EMISSION SIGNAL BASED ON WAVELET DECOMPOSITION

GEZHOU QIN[1], MING LI[2], SAIYIN FANG[1], TINGTING DENG[1], CHANGLIN HUANG[1], ZHOULING YANG[1], FEILONG MAO[1], YUE ZHAO[1]

[1]SOUTHWEST FORESTRY UNIVERSITY, CHINA
[2]ANHUI POLYTECHNIC UNIVERSITY, CHINA

(RECEIVED JUNE 2022)

ABSTRACT

Artificial AE sources were generated on the surfaces of *Ulmus pumila*, *Zelkova schneideriana*, *Cunninghamia lanceolata*, and *Pinus sylvestris var. mongolica* Litv. specimens. The AE transverse wave signal was decomposed into 3-layers detail signals by wavelet decomposition and reconstructed, and it was calculated based on correlation analysis. Then the longitudinal wave speed was calculated according to the time-difference-of-arrival (TDOA) method, and the wood dispersion phenomenon was studied. The results showed that the dispersion phenomenon of *Ulmus pumila* was obvious. The propagation speed of high-frequency signal was 2.38 times that of low-frequency signal. The ratio of high and low frequency propagation speed of soft wood was 1.72 and 1.73. The dispersion degree of *Zelkova schneideriana* was the weakest, and the propagation speed of the high frequency was 1.25 times of the low one. The ratios of longitudinal and transverse wave speeds of the four specimens were 4.59, 4.07, 4.24 and 4.2, respectively.

KEYWORDS: Wood, acoustic emission, frequency dispersion, propagation speed, wavelet analysis.

INTRODUCTION

As one of the most important natural resources in the world, wood has always accompanied human production and life, and has a wide range of applications, especially in construction. Acoustic emission (AE) refers to the phenomenon of instantaneous release of energy in the form of elastic waves in local areas of materials under the influence of internal or external forces (Baensch et al. 2015, Dai et al. 2001). Acoustic emission technology (AET) is a technology that uses piezoelectric ceramic sensors to transform the elastic wave signal generated by the AE source in the material into an electrical signal, and then uses instruments to amplify and process the electrical signal to obtain the characteristic parameters of the AE source (Yang and Ma 2006). AET can detect the changes of internal and surface elastic waves of materials, monitor the materials in real time. It can also determine the damage location based on the acoustic emission source localization technique, which has been widely used in the fields of metals, rocks, composite materials, etc. (Al-Dossary et al. 2009, Zhang et al. 2015, Jia et al. 2022).

In recent years, AET has been gradually applied in the field of wood damage location. Ju et al. (2018) used wavelet analysis to analyze the AE signals on the surface of horsetail glued laminated wood, which showed that there were significant differences in propagation speeds in both down-grain and cross-grain directions, and also indicated that wood structural changes, propagation characteristics and air medium had significant effects on AE signals. Wang et al. (2021) used two methods of PLB (pencil-lead break) and breaking thin wood strip tests to generate simulated AE sources in *Pinus sylvestris var.* mongolica Litv. and *Zelkova schneideriana*, respectively, and studied the propagation speeds of different simulated AE sources by wavelet processing and signal correlation analysis, and the results showed that the breaking thin wood strip test method was more objective in studying the AE signal propagation speeds. Li et al. (2021) used wavelet analysis to decompose and reconstruct the AE signal, and used the reconstructed AE signal to calculate the propagation speed in *Pinus sylvestris var.* mongolica Litv., and determined the effective frequency band of AE signal propagation on the surface and inside of *Pinus sylvestris var.* mongolica Litv. Li et al. (2021), Li and Xu (2019) showed that the time domain waveform amplitude of the AE signal tended to decay as the moisture content (MC) increased, the average speed of AE signal propagation on the specimen surface was inversely proportional to MC, and the average acoustic speed was maximum in absolute dry state. Li et al. (2020) found that the change of MC had a significant effect on the propagation speed and energy of AE signal in wood. Li et al. (2021) showed that the propagation speed of longitudinal and transverse wave of AE signal was greatly affected by the propagation medium, and the longitudinal wave mainly propagates along the cell wall of wood fiber cells, which was less hindered by the medium, and its propagation speed was about 4.6 times that of transverse wave. Ding et al. (2021) showed that in the linear localization of AE sources on wood surfaces, the accuracy of the linear localization algorithm for AE sources on wood can be significantly improved by performing singular spectrum analysis (SSA) noise reduction on the original AE signals and determining the signal propagation speed based on signal correlation analysis methods. Shen et al. (2015) Based on the triangular geometry localization principle of TDOA, proposed a method to locate the wood surface acoustic emission source, and the results showed that the method can determine the wood surface acoustic emission source location with high accuracy. In addition, AET has also been used in wood thermal modification; mechanical property test and identification of wood crack characteristics and other studies (Nasir et al. 2019, Nasir et al 2019, Garcia et al. 2012, Hernández et al. 2014, Lamy et al. 2015, Zhao et al. 2020, Hu and Zhang 2022).

However, the current calculation of the propagation speed of AE signals in wood is mostly for its group speed, and wood is an anisotropic material with the characteristics of composite and porous materials, and its physical properties in all directions are significantly different (Zhao et al. 2011). AE signals are mainly propagated in wood in the forms of longitudinal and transverse wave, transverse wave has more complex frequency distribution while longitudinal wave is relatively stable, and the AE signal in longitudinal wave is mainly low frequency components (Li et al. 2021). When the AE transverse wave signal propagates in wood, its high and low frequency signal speeds may vary greatly and there is a phenomenon of frequency dispersion. When there is dispersion, the wave packets composed of different frequency components will disperse, causing distortion of the received signal waveform relative to the transmitted signal, which will affect the accuracy of AE source localization technology. For this reason, *Ulmus pumila*, *Zelkova schneideriana*, *Cunninghamia lanceolata* and *Pinus sylvestris var.* mongolica Litv. were used to make specimens respectively, and the original AE signals of longitudinal and transverse wave were obtained by PLB tests on the right end face and upper surface of the specimens based on the AE signal high-speed acquisition system, and the wavelet analysis and correlation analysis were used to obtain the high and low frequency signal propagation speed of the AE transverse wave signal, exploring the dispersion effect of AE signals in different woods. Then, TDOA was used to calculate the longitudinal wave speed and compare it with transverse wave speed.

MATERIALS AND METHODS

Test materials

The difference of wood microstructure can obviously affect the propagation characteristics of the AE signal. Therefore, *Ulmus pumila* and *Zelkova schneideriana* belong to hard wood. *Cunninghamia lanceolata and Pinus sylvestris* var. mongolica Litv. belong to soft wood. For ease of description, *UP*, *ZS*, *CL* and *PS* are used to represent *Ulmus pumila*, *Zelkova schneideriana*, *Cunninghamia lanceolata* and *Pinus sylvestris var.* mongolica Litv., respectively. The size of all specimens was 800 mm (length) × 60 mm (width) × 30 mm (thickness). The densities of the four specimens were 0.622 $g\cdot cm^{-3}$, 0.613 $g\cdot cm^{-3}$, 0.496 $g\cdot cm^{-3}$, and 0.472 $g\cdot cm^{-3}$, respectively.

Test equipment

In order to obtain complete original AE signal waveform data, a 3-channel signal acquisition system was built based on NI USB-6366 high-speed acquisition card and Lab VIEW acquisition program. The sensor is an SR-2A piezoelectric ceramic sensor with a bandwidth of 50~400 kHz and a 40 dB gain preamplifier. Relevant research shows that the frequency of the wood's AE signal is mainly distributed in the range of 50 kHz ~ 200 kHz (Li et al. 2018, Zhang et al. 2016, Li et al. 2019). According to Shannon's sampling theorem, the sampling frequency of each channel of the AE signal acquisition system was set to 500 kHz, and the output voltage of the amplifier ranged from -5 to 5 V.

Test methods

Simulated AE source was generated by PLB test. To ensure the consistency of the AE source, a 0.5 mm diameter pencil core was placed at 30° to the surface of the specimen at a distance of 2.5 mm from the contact point and the PLB test was carried out according to ASTM E976-2015. In the test, three sensors were equally spaced on the upper surface of the specimens, S_1 sensor was 100 mm from the right end face of the specimen, and the distance between sensors S_2 and sensor S_1 was 300 mm (Fig. 1).

Since the AE signal generated by the PLB was a burst type signal, the signal characteristics were characterized by short duration and weak energy, resulting in the AE signal being submerged by the noise signal, and the original signal cannot be directly used to characterize the propagation characteristics of the AE signal. Therefore, wavelet analysis was used to process the AE signal. The two-point TDOA method was used to determine the transverse wave propagation speed of the AE signal. According to $v = \Delta s/\Delta t$, the distance between the two sensors in the test was known $\Delta s = 300\ \mathrm{mm}$, and only the time difference Δt between the two sensors is needed to calculate the propagation speed of the AE signal. The time difference Δt can be solved by using the inter-correlation function, and for the two random signals $x(t)$ and $y(t)$, the inter-correlation function $R_{xy}(\tau)$ between them is defined as in Eq. 1:

$$R_{xy}(\tau) = \lim_{T\to\infty}\frac{1}{T}\int_0^T x(t)\, y(t+\tau)\, dt\# \tag{1}$$

where: the intercorrelation function can characterize the similarity of two signals, τ represents the translation units of the signal on the time axis and T is the initial signal length.

In Eq. 1, when $\tau = \tau_0$, $|R_{xy}(\tau)|$ obtains the maximum value, it means that the signal $y(t)$ has the highest similarity with the signal $x(t)$ after translating τ_0 units on the time axis. Therefore, the correlation function can be used to analyze the AE signal and the time difference Δt between the AE signal arriving at the two sensors can be found, and the propagation speed v of the specimen can be calculated. According to the elastic wave theory, it is known that the longitudinal wave speed is much larger than the transverse wave speed, and the TDOA method was used to find the longitudinal wave speed.

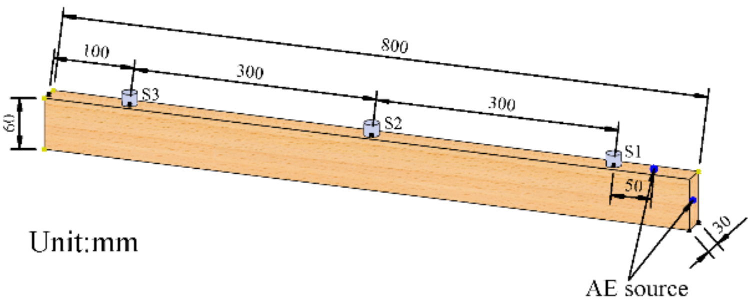

Fig. 1: Test diagram.

Wavelet processing

Wavelet analysis has good time-frequency analysis characteristics, which can decompose the original AE signal into different frequency bands to obtain signals with different frequency components, and it can filter the ultra-low frequency signal, which can better remove the noise and retain the AE signal. while filtering out the ultra-low frequency signal, which can better remove the noise, while the acoustic emission signal is retained.

In order to improve the frequency domain localization capability of wavelet analysis, the original AE signal was decomposed by the Daubechies (db10) wavelet basis function with high vanishing moments and good regularity, and the system sampling frequency was 500 kHz. According to Shannon's sampling theorem, the maximum frequency that can be detected in theory is 250 kHz. Based on the wavelet transform multi-scale analysis theory, the three-layer detail signals obtained after wavelet analysis are (250 kHz ~ 125 kHz), (125 kHz ~ 62.5 kHz), and (62.5 kHz ~ 31.25 kHz), while the frequency of wood AE signals is mainly distributed in 50 kHz ~200 kHz, covering the frequency range of AE signals.

RESULTS AND DISCUSSION

Analyzing the propagation characteristics of AE signals is the key to Nondestructive Testing (NDT) using AET technology. It is of great significance to study the characteristics of acoustic emission signals, transverse wave speed and longitudinal wave speed of different wood for wood damage location and wood identification. Because wood is an orthotropic material, the propagation speed of AE signal in the vertical grain direction and along grain direction is different. Studying the characteristics of acoustic emission signals and transverse and longitudinal wave speeds of different woods is of great significance for wood damage localization and wood identification.

Acoustic emission transverse wave signal characteristics

The AE signal longitudinal wave waveforms of the four specimens are shown in Figs. 2-5, and the AE signals collected by S_1, S_2, and S_3 sensors are shown from top to bottom in the figure. Because the AE signal generated by the PLB is a burst type signal with a short duration, the data points with a duration of 8 ms were intercepted to analyze the AE signal. The signal attenuation and the changes of high and low frequency components can be analyzed from the waveform diagram. In the diagram, the AE signal waveforms in *UP* and *ZS* S_1 sensors are dense in the early stage, mainly high-frequency signals, while the waveforms of the AE signals in the sensors of S_2 and S_3 are sparse and mainly low frequency components. AE signal waveforms in S_2 and S_3 sensors are sparse and mainly composed of low-frequency components. In the S_2 and S_3 sensors of *CL* and *PS,* the early waveform of AE signal was significantly more dense than that of *UP* and *ZS*. It can be known that the attenuation of AE high-frequency signal in hard wood was significantly faster than that of soft wood. The AE signal amplitude decreased significantly in the four specimens from S_1 to S_2, and the AE signal attenuation was relatively small in the S_2 and S_3 sensors. As wood is a kind of viscoelastic medium with strong viscosity, and when the AE signal propagates in wood, the high-frequency component decays rapidly due to the influence of wood viscosity and other factors(Wang et al. 2021), because the density of hard wood is larger than that of soft wood, and the viscosity is stronger, so the high-frequency component decays more rapidly when the AE signal propagates in hard wood. In the late stage of AE signal propagation, because the high-frequency component decays rapidly, the AE signal is mainly dominated by low-frequency components, and the low-frequency signal decays slowly, so the AE signal amplitude collected by S_2, S_3 sensors changes little.

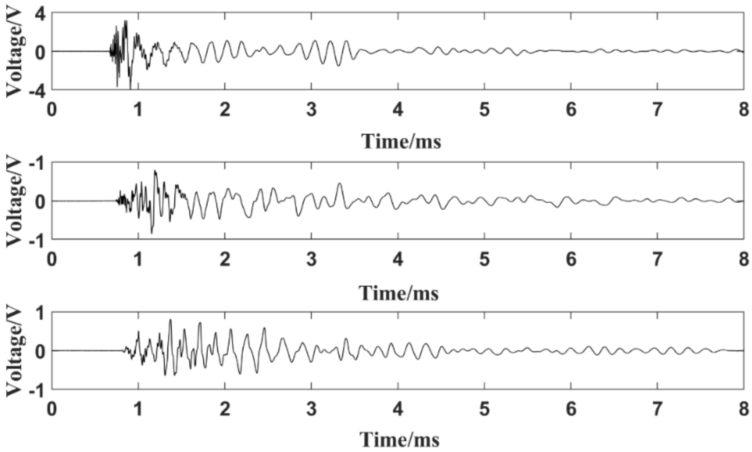

Fig. 2: Original AE signal waveform of Ulmus pumila.

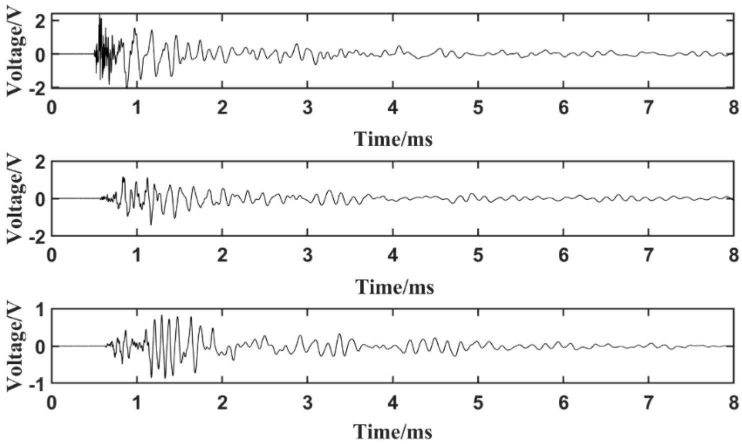

Fig. 3: Original AE signal waveform of Zelkova schneideriana.

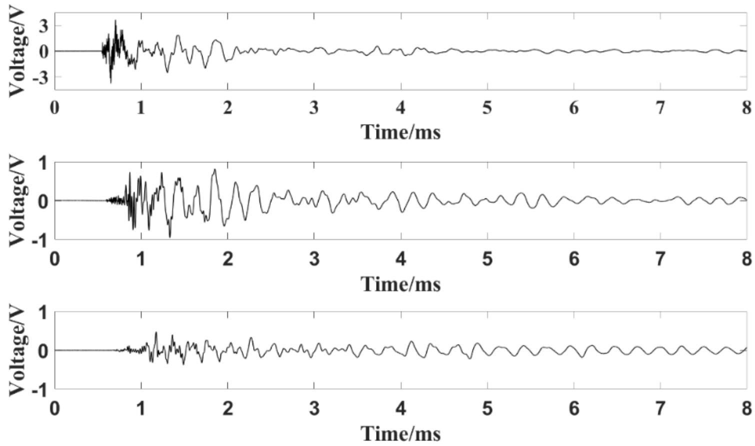

Fig. 4: Original AE signal waveform of Cunninghamia lanceolata.

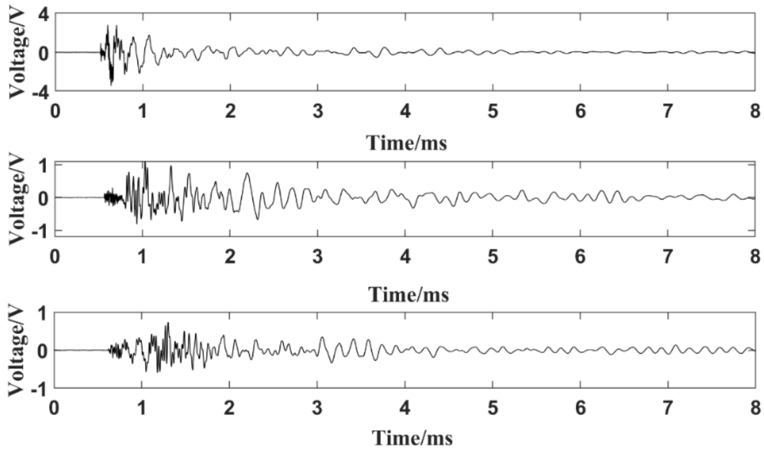

Fig. 5: Original AE signal waveform of Pinus sylvestris var. mongolica Litv.

In order to study the frequency dispersion characteristics of the AE signal, the original AE signals were decomposed in three layers based on wavelet decomposition, as shown in Figs. 6 and 7, the detailed signal frequency domain diagrams of the first, second and third layers of AE signal wavelet decomposition are shown from top to bottom. It can be seen from the figure that the frequency distributions of the four specimens are similar, and the frequency components of first layer signal are relatively single, mainly in 163.1 kHz ~ 166 kHz, the second layer signal center frequency is 71.29 kHz ~ 87.89 kHz, and the third layer signal main frequency is concentrated in 36.13 kHz ~ 39.06 kHz. When PLB tests are performed on wood, AE signals of different frequencies are excited, however, due to the viscosity of wood and its internal porous structure, some frequencies of AE signals can be filtered when they are transmitted in wood. It can be seen from the figure that the frequencies of AE signals are mainly distributed in the above three frequency bands, and there is basically no difference in the frequency distribution of AE signals in hardwood and soft wood.

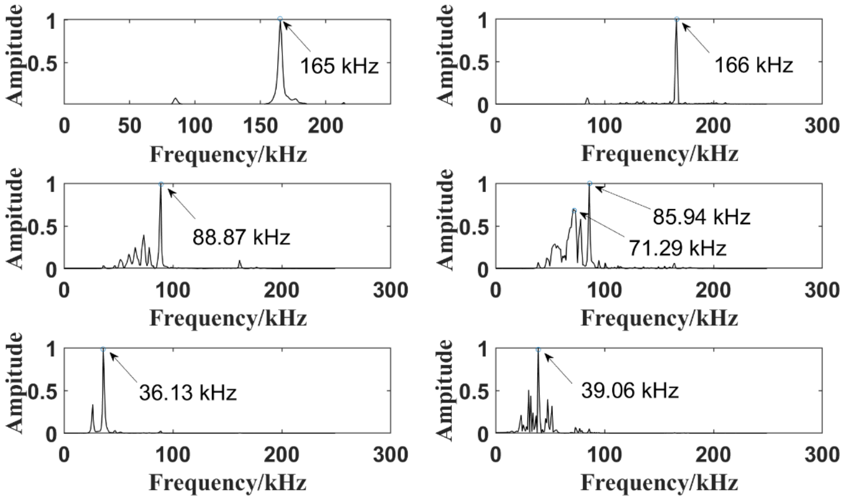

Fig. 6: Frequency domain diagram of wavelet decomposition detail signal of hard wood.

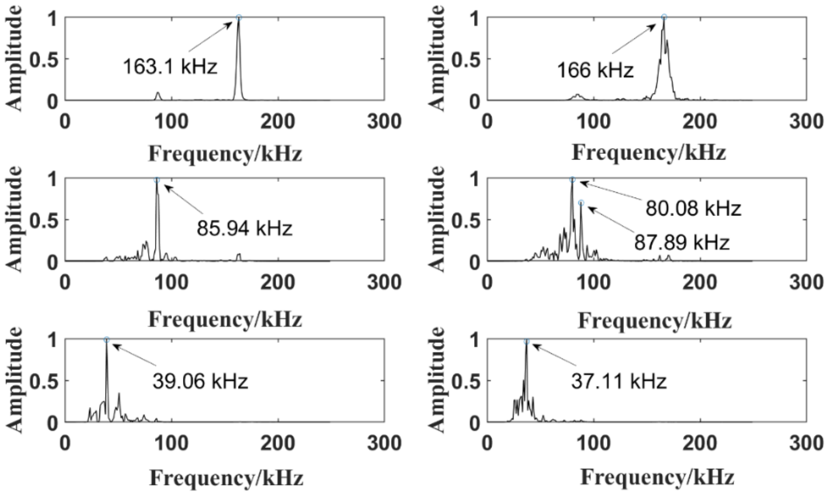

Fig. 7: Frequency domain diagram of wavelet decomposition detail signal of soft wood.

Comparative analysis of AE signal propagation speed

The test was based on correlation analysis to calculate the speed of each layer detail signal, reconstructed signal and original signal. In order to eliminate the contingency of test results, the results in the following table are averaged from 10 groups of test data. Tab. 1 shows the transverse wave speed of two hard wood, *UP* and *ZS*, and Tab. 2 shows the transverse wave speed of two soft wood of *CL* and *PS*. Due to the fast attenuation of high-frequency signals. The AE signal of S_1 and S_2 sensor were used to calculate the propagation speed of high-frequency signals. The attenuation of low-frequency signal is slow. If the correlation analysis is adopted, the distance is too close, which may cause large errors, so the AE signals of S_1 and S_3 sensors were used to calculate the speed.

Tab. 1: Specimen transverse wave speed.

Wood species	Speed ($m \cdot s^{-1}$)				
	v_{1-12}	v_{2-13}	v_{3-13}	v_{R-13}	v_{O-13}
Ulmus pumila	2200	930	922	910	864
Zelkova schneideriana	1437	1100	1200	1191	815
Cunninghamia lanceolata	2131	1228	1246	1263	947
Pinus sylvestris var. mongolica Litv.	2209	1265	1302	1228	636

Note: V_{x-ij} -*x* is the number of wavelet decomposition layers, *i* and *j* are the sensor number, *R* is the reconstructed signal, and *O* is the original signal.

As shown in Tab. 1, the propagation speed of high-frequency signal in the first layer is significantly higher than that of intermediate frequency signal in the second layer and low-frequency signal in the third layer. The signal speed of elm in the first layer is 2.38 times that of the second and third layers. The propagation speed of high frequency signal of *ZS* is 1.25 times that of medium and low frequency signal. And it is 1.72 times and 1.73 times in *CL* and *PS* specimens, respectively. In each specimen, the dispersion of *UP* was serious, that of *ZS* was weak, and the ratio of high and low frequency signal propagation speed of *CL* and PS was similar, and the frequency dispersion of the two soft woods was the same. The results shows that there are different degrees of dispersion in different woods. It can be seen that the propagation speed of the second layer and third layer detail signal is close to that of the reconstructed signal, which is because the high-frequency components decay rapidly during the propagation process in the specimen, and the AE signal in the later stage of propagation is basically dominated by the medium and low-frequency components. Moreover, the second layer signal accounts for a relatively small proportion of the whole AE signal (Ju et al. 2018, 2019), which propagates more stably, and the third layer is dominated by low-frequency signals, so the speeds of the three are similar. Due to the influence of the noise and the standing wave signal, the propagation speed of the original AE signal is less than that of the reconstructed AE signal. Based on wavelet decomposition and noise reduction, Li et al. (2021) used correlation analysis to obtain that the transverse speed of *PS* is 1377.6 $m \cdot s^{-1}$. Wang et al. (2021) generated the simulated AE source by PLB tests and calculated the average propagation speed of AE signal in *ZS* as 1120.5 $m \cdot s^{-1}$. This paper calculated the average speed of original AE signal in *PS* as 1228 $m \cdot s^{-1}$ and the average speed of original AE signal in *ZS* as 1191 $m \cdot s^{-1}$. The average speed of AE signal was 1191 $m \cdot s^{-1}$ in *ZS* which is the same as the results of the above results.

After applying wavelet decomposition, the transverse wave speeds of AE signals in different frequency bands can be calculated based on correlation analysis, which can not only analyze the dispersion of wood, but also reduce the impact of noise and standing wave on AE signals, and accurately calculate the speed. Based on the TDOA method, the distance Δx and time difference Δt between sensors are known, and the longitudinal wave speed can be obtained by using $v = \Delta x / \Delta t$. As shown in Tab. 2, the longitudinal wave speeds of the AE signals of *UP*, *ZS*, *CL* and *PS* are 4172 $m \cdot s^{-1}$, 4849 $m \cdot s^{-1}$, 5357 $m \cdot s^{-1}$ and 5159 $m \cdot s^{-1}$, respectively. Through comparative analysis, the ratio of longitudinal wave and transverse wave speeds is stable within a certain range., and the longitudinal wave speed of *UP* is 4.59 times the transverse wave speed of the reconstructed signal. The longitudinal wave speed of *ZS* is 4.07 times that of the transverse wave, which is 4.07 times and 4.24 times in *CL* and *PS,* respectively. The longitudinal wave speed of *PS* is 4.2 times that of the transverse wave. Relevant studies (Ding et al. 2021, Li et al. 2021) showed that the longitudinal wave speed of *PS* and *ZS* was about 4.6 times that of the transverse wave speed. The longitudinal and transverse wave speed ratios of the four specimens in this paper are 4.07 – 4.20. Considering the calculation error and difference of the specimens, the results obtained in this paper are consistent with the above research results. This is because the longitudinal wave signal propagates along the grain direction in the wood, which is consistent with the arrangement direction of wood cells. When the AE signal propagates along the fiber direction, it will accelerate the attenuation of high frequency components (Wang et al. 2020), so the longitudinal wave mainly propagates in low-frequency components, and the low-frequency attenuation is slow. Relatively speaking, the longitudinal wave is a more stable signal wave.

Tab. 2: Longitudinal wave speed of specimen.

Test material	Δt (μs)	v ($m \cdot s^{-1}$)
Ulmus pumila	71	4172
Zelkova schneideriana	62	4849
Cunninghamia lanceolata	56	5357
Pinus sylvestris var. mongolica Litv.	58	5159

CONCLUSIONS

Based on wavelet decomposition, the AE transverse wave signals of four specimens were decomposed in 3-layer and reconstructed, then the transverse wave transmission speeds of three layers of detail signals, reconstructed AE signals and original AE signals are obtained by correlation analysis. Through the study on the frequency domain diagram of the detail signal of the specimen, it is found that the AE signal is mainly distributed in three frequency bands (163.1 kHz ~166 kHz), (71.29 kHz ~87.89 kHz) and (36.13 kHz~39.06 kHz). The calculation results shows that the reconstructed AE signal speed is closer to the low-frequency speed, and the calculated speed is more reliable than the original AE signal propagation speed. By comparing the high and low- frequency speeds, the ratio of high and low-frequency speeds of *UP* is 2.38, the ratio of high and low- frequency speeds of *ZS* is 1.25, and it is 1.72 and 1.73 in *CL* and *P*S, respectively. It was found that there are frequency dispersion phenomena in different degrees in each specimen. Because there is a great difference between the high and low frequency transverse wave speeds of wood, this will have a greater impact on the accuracy of AE source localization technology. Therefore, the dispersion effect should be considered when AE signal transverse wave is used to locate AE source of wood in the future. The TDOA method was used to calculate the longitudinal wave speed. By comparing the longitudinal wave speed and longitudinal wave speed of the AE signal, it is calculated that the ratio of transverse wave speed to transverse wave speed of *UP* is 4.59, and it is 4.07, 4.24, 4.2 in *ZS*, *CL*, and *PS,* respectively. The results show that the speed ratio of longitudinal wave and transverse wave of wood is stable within a certain range, and because the transverse wave mainly propagates at low frequency, it is a kind of relatively stable wave, which provides a reference for the comparative analysis of AE source location technology using transverse wave and transverse wave.

At present, there are few studies on the dispersion characteristics of wood AE signal. In this study, the propagation speed of AE signal in wood is calculated based on wavelet decomposition, correlation analysis and TDOA method, and the propagation speed of high and low-frequency signals, transverse wave and transverse wave speeds in wood are compared and analyzed, aiming to broaden the research direction of AE source localization technology.

Because there is modal mixing in wavelet decomposition, which has an impact on the calculation accuracy of propagation speed, it is worth further research on how to avoid the mixing phenomenon when extracting and analyzing the single frequency band of AE signal in the future.

ACKNOWLEDGEMENTS

The authors are grateful for the support of the China Natural Science Foundation (NO: 32160345, 31760182) and Department of Education of Yunnan Provincial (NO: 2021J0156, NO: 2021J0158). Start up fund for introducing talents and scientific research of Anhui University of Engineering (NO: 2021YQQ037).

REFERENCES

1 Al-Dossary, S., Hamzah, R.R., Mba, D., 2009: Observations of changes in acoustic emission waveform for varying seeded defect sizes in a rolling element bearing. Applied Acoustics 70(1): 58-81.

2 Baensch, F., Zauner, M., Sanabria, S.J., Sause, M.G., Pinzer, B.R., Brunner, A.J., Niemz, P., 2015: Damage evolution in wood: synchrotron radiation micro-computed tomography (SRμCT) as a complementary tool for interpreting acoustic emission (AE) behavior. Holzforschung 69(8): 1015-1025.

3 Dai, G., Xu, Y.T., Li, W., Zhang, Y., 2001: Application and study of acoustic emission technology(AET). Journal of Daqing Petroleum Institute 25(03): 95-98.

4 Ding, R., Luo, R.H., Lai, F., Wang, M.H., Deng, T.T., Luo, T.F., Li, M., 2021: Straight line location algorithm of wood acoustic emission source based on singular spectrum analysis and signal correlation analysis methods. Journal of Northwest Forestry University 36(05): 173-178+245.

5 Garcia, R.A., de Carvalho, A.M., de Figueiredo Latorraca, J.V., de Matos, J.L.M., Santos, W.A., de Medeiros Silva, R.F., 2012: Nondestructive evaluation of heat-treated *Eucalyptus grandis* Hill ex Maiden wood using stress wave method. Wood Science and Technology 46(1): 41-52.

6 Hernández, R.E., Passarini, L., Koubaa, A., 2014: Effects of temperature and moisture content on selected wood mechanical properties involved in the chipping process. Wood Science and Technology 48(6): 1281-1301.

7 Hu, W., Zhang, J., 2022: Effect of growth rings on acoustic emission characteristic signals of southern yellow pine wood cracked in mode I. Construction and Building Materials 329: 127092-127105.

8 Jia, H., Zhang, L.A., Wang, J.H., Huang, X.M., Yu, L.F., 2022: Damage pattern recognition of wind turbine blade composite material based on acoustic emission technology. Renewable Energy Resources 40(01): 67-72.

9 Ju, S., Li, X.C., Luo, T.F., Li, M., 2018: Characteristics of acoustic emission signals on the surface of Masson pine glulam with wavelet analysis method. Journal of Northeast Forestry University 46(08): 84-90.

10 Ju, S., Li, X.C., Luo, T.F., Li, M., 2019: Anisotropic propagation of acoustic emission signal on surface of *Pinus massoniana* Lamb. glulam. China Forestry Science and Technology 4(02): 48-53.

11 Lamy, F., Takarli, M., Angellier, N., Dubois, F., Pop, O., 2015: Acoustic emission technique for fracture analysis in wood materials. International Journal of Fracture 192(1): 57-70.

12 Li, M., Wang, M.H., Ding, R., Deng, T.T., Fang, S.Y, Lai, F., Luo R.H., 2021: Study of acoustic emission propagation characteristics and energy attenuation of surface transverse wave and internal longitudinal wave of wood. Wood Science and Technology 55(6): 1619-1637.

13 Li, X.C., Ju, S., Luo, T.F., Li, M., 2020: Effect of moisture content on propagation characteristics of acoustic emission signal of *Pinus massoniana* Lamb. European Journal of

Wood and Wood Products 78(1): 185-191.
14 Li, Y, Xu, F., 2019: Signal processing and identification on the surface of *Pinus massoniana* Lamb. glulam using acoustic emission and improvement complete ensemble empirical mode decomposition with adaptive noise. Measurement 148: 106978-106992.
15 Li, Y., Yu, S.S., Dai, L., Luo, T.F., Li, M., 2018: Acoustic emission signal source localization on plywood surface with cross-correlation method. Journal of Wood Science 64(2): 78-84.
16 Nasir, V., Cool, J., Sassani, F., 2019: Acoustic emission monitoring of sawing process: artificial intelligence approach for optimal sensory feature selection. The International Journal of Advanced Manufacturing Technology 102(9): 4179-4197.
17 Nasir, V., Nourian, S., Avramidis, S., Cool, J., 2019: Stress wave evaluation for predicting the properties of thermally modified wood using neuro-fuzzy and neural network modeling. Holzforschung 73(9): 827-838.
18 Shen, K.N., Ding, X.Z., Zhao, H.L., Li, M., 2015: Acoustic emission signal source localization in wood surface with triangle positioning method. Journal of Northeast Forestry University 43(04): 77-81+112.
19 Wang, M.H., Deng, T.T., Fang, S.Y., Li, X.S., Lai, F., 2021: Generation and characteristics of simulated acoustic emission source of wood. Journal of Northeast Forestry University 49(06): 96-101+118.
20 Wang, M.H., Deng, T.T., Ju, S., Li, X.C., Li, M., 2020: Effect of wood surface crack on acoustic emission signal propagation characteristics. Journal of Northeast Forestry University 48(10): 82-88.
21 Wang, M.H., Deng, T.T., Li, X.S., Ding, R., Lai, F., Luo, R.H., Li, M., 2021: Propagation characteristics of acoustic emission signals in l-shaped wood. Journal of Northwest Forestry University 36(02): 213-219.
22 Yang, R.F., Ma, T.H., 2006: A study on the applications of acoustic emission technique. Journal of North University of China (05): 456-461
23 Li, X.C., Ju, S., Luo, T.F., Li, M., 2019: Influence of adhesive layer at Masson pine glulam on acoustic emission signal propagation characteristics. Journal of Northwest Forestry University 34(03): 185-190+239.
24 Li, X.S., Deng, T.T., Wang, M.H., Luo, R.H., 2021: Frequency domain identification of acoustic emission signals on surface and interior of *Pinus sylvestris* var. mongolica based on wavelet analysis. Journal of Northwest Forestry University 36(04): 209-213+288.
25 Li, Y., Xu, F, Y., 2019: Acoustic emission signal characteristics of *Pinus yunnanensis* with different moisture content. Scientia Silvae Sinicae 55(06): 96-102.
26 Zhang, C., Liang, W., Li, Z., Xu, S., Zhao, Y., 2015: Observations of acoustic emission of three salt rocks under uniaxial compression. International Journal of Rock Mechanics and Mining Sciences 77: 19-26.
27 Zhang, P., Li, M., Wang, R., Jiang, Y., 2016: Acoustic emission research of wood-power blades composites in three point bending test. Engineering Plastics Application 44(4): 21-26.
28 Zhao, Q., Zhao, D., Zhao, J., 2020: Thermodynamic approach for the identification of

instability in the wood using acoustic emission technology. Forests 11(5): 534-554.
29 Zhao, R., Cheng, X., Sun, J., Wang, X., Fei, B., 2011: Study on the longitudinal tensile strength of the tracheids of soft wood. Journal of Anhui Agricultural University 38(4): 491-495.

GEZHOU QIN, SAYIN FANG, TINGTING DENG, CHANGLIN HUANG,
ZHOULING YANG, FEILONG MAO, YUE ZHAO
SOUTHWEST FORESTRY UNIVERSITY
SCHOOL OF MACHINERY AND TRANSPORTATION ENGINEERING
KUMMING 650224
CHINA
*Corresponding author: swfu_lm@swfu.edu.cn

MING LI[1,2]
ANHUI POLYTECHNIC UNIVERSITY
[1]KEY LABORATORY OF ADVANCED PERCEPTION AND INTELLIGENT CONTROL
OF HIGH-END EQUIPMENT OF MINISTRY OF EDUCATION
[2]SCHOOL OF ELECTRICAL ENGINEERING
ANHUI 241000
CHINA